



# The Imaging Performance of Preclinical Ultrasound Scanners Using the Edinburgh Pipe Phantom

Carmel M Moran<sup>1\*</sup>, Christopher McLeod<sup>2</sup>, Karne McBride<sup>2</sup>, Scott Inglis<sup>2</sup>, Adrian JW Thomson<sup>1</sup> and Stephen D Pye<sup>1,2</sup>

<sup>1</sup>Centre for Cardiovascular Science, Queen's Medical Research Institute, University of Edinburgh, Edinburgh, United Kingdom, <sup>2</sup>Medical Physics, NHS Lothian, Edinburgh, United Kingdom

## OPEN ACCESS

### Edited by:

Simo Saarakkala,  
University of Oulu, Finland

### Reviewed by:

George Corner,  
University of Dundee, United Kingdom  
Jacinta Browne,  
Mayo Clinic, United States  
Christian Kollmann,  
Medical University of Vienna, Austria

### \*Correspondence:

Carmel M Moran  
carmel.moran@ed.ac.uk

### Specialty section:

This article was submitted to  
Medical Physics and Imaging,  
a section of the journal  
Frontiers in Physics

**Received:** 17 January 2022

**Accepted:** 25 April 2022

**Published:** 26 May 2022

### Citation:

Moran CM, McLeod C, McBride K, Inglis S, Thomson AJW and Pye SD (2022) The Imaging Performance of Preclinical Ultrasound Scanners Using the Edinburgh Pipe Phantom. *Front. Phys.* 10:802588. doi: 10.3389/fphy.2022.802588

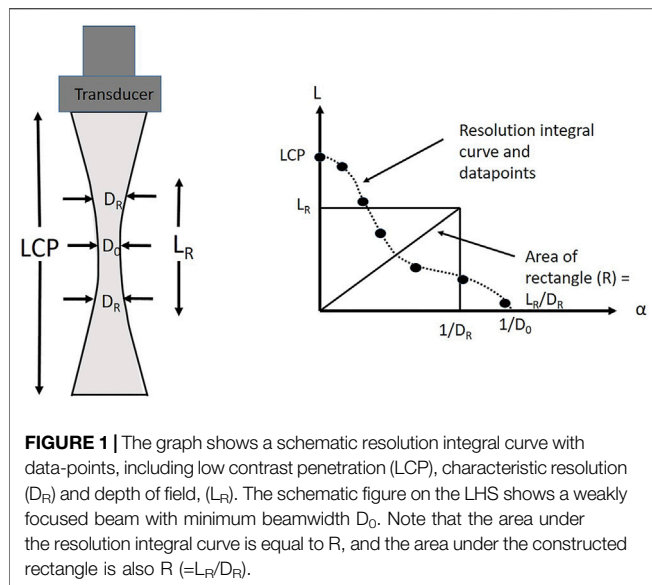
The greyscale imaging performance of a total of 17 preclinical transducer/scanner combinations were measured over a period of 10 years. These comprised nine single element transducers and eight array transducers with nominal central frequencies ranging between 15 and 55 MHz, and were from four commercially-available preclinical ultrasound scanners. Performance was assessed using a single figure of merit, the resolution integral, using measurements acquired from images of a test-object, the Edinburgh Pipe Phantom. Two further parameters were derived from the resolution integral: *characteristic resolution* and *depth-of-field*. Our results demonstrate that 1) resolution integral values of the array transducers were greater than single-element transducers, and 2) the array transducers demonstrated greater depths of field than the single-element transducers of the same nominal frequency. Moreover we demonstrate that use of this single figure-of-merit enabled identification and quantification of changes in imaging performance of preclinical transducers over a 10-years period.

**Keywords:** ultrasound, preclinical, imaging, performance, Edinburgh Pipe Phantom

## INTRODUCTION

Preclinical ultrasound is a real-time imaging technique providing high resolution data on soft tissue structures within small animals. The footprint of a preclinical ultrasound scanner is typically less than 1 m<sup>2</sup> and even with a scanning platform and anaesthetic rig, its space requirements are relatively small compared to other preclinical imaging techniques such as magnetic resonance imaging (MRI) and positron emission tomography (PET) scanners. Moreover, the lack of ionising radiation has resulted in preclinical ultrasound scanners becoming a key component of biological research facilities where they are used to phenotype animals and monitor the serial progression of disease. To ensure robust imaging data sets are obtained, regular measurement and monitoring of the imaging performance of these scanners is important, especially if degradation in imaging performance is gradual rather than a step-change. However, the commercial test-objects that are routinely used to measure the performance of clinical ultrasound scanners do not have sufficiently small targets to adequately measure the imaging performance of these high resolution preclinical scanners. In addition, commercial test-objects are composed of tissue-mimicking materials (TMM), designed and manufactured to acoustically mimic soft tissue at frequencies routinely used in clinical imaging. These materials are often uncharacterised at frequencies greater than 20 MHz [1, 2].

More recently several groups have developed in-house test-objects, with small targets embedded within them to measure the imaging performance of high frequency transducers and scanners. One



such example describes the development of a novel anechoic-sphere phantom with spheres of diameters between 0.10 and 1.09 mm embedded into slabs of TMM [3]. This enabled a comparison of the imaging performance of an in-house 40 MHz annular array transducer and two commercial 40 MHz transducers. Another approach used two 0.3 mm diameter monofilaments to measure a single figure of merit based on lateral resolution and used this to assess clinical scanners up to 15 MHz [4]. Our group previously reported the use of the Edinburgh Pipe Phantom (EPP) to measure the imaging performance of both clinical and high resolution preclinical ultrasound scanners using a single figure-of-merit called the resolution integral (R) [5–7]. We demonstrated the ability of this parameter to differentiate between transducers for different clinical applications and to detect changes in imaging performance [8, 9]. To measure the resolution integral of preclinical ultrasound scanners, a variation of the EPP test object, was manufactured in-house [10]. The phantom consists of a perspex box containing a block of agar-based TMM [11], within which a series of cylinders (pipes) of diameters ranging from 350  $\mu\text{m}$  to 8 mm and angled at 40° to the vertical were moulded during the manufacturing process.

Once the agar had set, the pipes were filled with fluid composed of water/glycerol and antibacterial solution with speed of sound 1540  $\text{ms}^{-1}$ . This fluid was also used to acoustically couple the transducer to the surface of the phantom. The addition of a series of smaller pipes down to 45  $\mu\text{m}$  diameter and characterization of the TMM up to 50 MHz [12, 13] extended the utility of the EPP to preclinical ultrasound scanners and provided a means to objectively assess the imaging performance of high resolution scanners using the resolution integral [14].

## Resolution Integral

The resolution integral is a dimensionless figure-of-merit and is defined as the ratio of the penetration depth of an ultrasound beam to

the ultrasound beam width in a particular medium. High performing transducers will be associated with large penetration depths and narrow beam widths resulting in large resolution integral values.

Measurement of the resolution integral using the EPP has been described elsewhere [6] and is briefly summarised here. The transducer is coupled to the surface of the EPP and an image of a pipe is centred in the scan-plane. The controls are optimised so that the pipe can be visualised as superficially as possible and the distance from the top of the pipe to the transducer surface is measured visually by the user. The lower section of the same pipe is then scanned, centred in the scan-plane and the image is again optimised to determine the maximum depth that the pipe can be visualised. The difference between these two measurements corresponds to the ordinate (y-value, L) of one data-point on the resolution integral graph (Figure 1). The abscissa value (x-value,  $\alpha$ ) is the reciprocal of the effective diameter of each pipe. The effective diameter is equal to the geometric mean of the pipe dimensions in the imaging and elevation plane and is equal to  $d/\sqrt{\cos 40^\circ}$  where d is equal to the diameter of the pipe. Pipes are scanned sequentially, with each pipe providing a data-point on the resolution integral graph. Finally, a low contrast penetration (LCP) measurement is taken within the TMM. The LCP depth is defined as the maximum depth at which speckle can be identified from system noise. The measurement is undertaken in real-time as it is easier to differentiate speckle from system noise. This value forms the intercept of the resolution-integral curve with the ordinate. The resolution integral is calculated as the area under the curve defined by these datapoints. Two additional parameters are also determined: the characteristic resolution ( $D_R$ ) and depth-of-field ( $L_R$ ). The depth-of-field defines a depth over which there is optimal resolution and the characteristic resolution represents the typical (characteristic) resolution within the depth-of-field. These two parameters are calculated from a rectangle, constructed with an identical area to the area under the resolution integral curve, such that the diagonal of the rectangle from the origin to the opposing corner bisects the area under the resolution integral curve. The intercept of the rectangle on the y-axis is the depth-of-field, and the intercept of the rectangle the x-axis is the characteristic resolution (Figure 1).

Typically, to calculate the resolution integral for each transducer, measurements of a minimum of 5 pipes and an LCP measurement are undertaken. Each data-point is the mean of 3 sets of measurements on each pipe. From this data, the resolution integral is calculated and the  $L_R$  and  $D_R$  values.

In this brief report, we present the results of the imaging performance of 17 preclinical transducers that have been assessed over the past 10 years using the resolution integral and its associated parameters.

## METHODS

All scanners and transducers (Table 1) were assessed within United Kingdom biological research facilities from 2010 to 2020 and all were in use with no visible faults. All but one of the transducers were manufactured by Fujifilm Visualsonics (Toronto, Canada) and

**TABLE 1** | Details of the 17 preclinical ultrasound transducers and their performance measurements. \* indicates data that was published previously [14]. Note that for three of the transducers, performance values, obtained in 2020 when the Vevo 770 scanner was decommissioned are also included.

| Scanner   | Transducer | Single element (SE) or linear array (LA) | Nominal central frequency (MHz) | Focal length (mm) | Resolution integral | Depth of field (mm) | Characteristic resolution ( $\mu\text{m}$ ) |
|-----------|------------|--|---------------------------------|-------------------|---------------------|---------------------|---|
| Vevo 770  | RMV716     | SE                                       | 17.5                            | 17.5              | 23 (2011)           | 12.3                | 549   |
| Vevo 770  | RMV710     | SE                                       | 25                              | 15                | 18 (2008)*          | 5.4                 | 289   |
| Vevo 770  | RMV707B    | SE                                       | 30                              | 12.7              | 23 (2008)*          | 5.3                 | 225   |
| Vevo 770  | RMV712     | SE                                       | 35                              | 9                 | 25 (2011)           | 5.9                 | 234   |
| Vevo 770  | RMV703     | SE                                       | 35                              | 10                | 22 (2011)           | 6.3                 | 287   |
| Vevo 770  | RMV704     | SE                                       | 40                              | 6                 | 25 (2010)*          | 3.6                 | 145   |
|           |            |  |                                 |                   | 21 (2015)           | 4.3                 | 202   |
|           |            |  |                                 |                   | 18 (2020)           | 5.1                 | 278   |
| Vevo 770  | RMV711     | SE                                       | 55                              | 6                 | 24 (2010)*          | 3.6                 | 145   |
|           |            |  |                                 |                   | 19 (2015)           | 3.5                 | 184   |
|           |            |  |                                 |                   | 17 (2020)           | 3.5                 | 202   |
| Vevo 770* | RMV708     | SE                                       | 55                              | 4.5               | 21 (2010)*          | 2.8                 | 131   |
|           |            |  |                                 |                   | 17 (2015)           | 3.5                 | 202   |
|           |            |  |                                 |                   | 19 (2020)           | 3.4                 | 184   |
| S Sharp   | PB406      | SE                                       | 40                              | 13                | 23 (2015)           | 4.3                 | 187   |
| Vevo2100  | MS200      | LA                                       | 15                              |                   | 58 (2009)*          | 32.2                | 559   |
| Vevo2100  | MS250      | LA                                       | 21                              |                   | 56 (2009)*          | 24                  | 430   |
| Vevo2100  | MS400      | LA                                       | 30                              |                   | 49 (2009)*          | 13.2                | 269   |
| Vevo2100  | MS550D     | LA                                       | 40                              |                   | 55 (2009)*          | 10.9                | 197   |
| Vevo2100  | MS550S     | LA                                       | 40                              |                   | 56 (2009)*          | 10.5                | 188   |
| Vevo3100  | MX201      | LA                                       | 15                              |                   | 45 (2019)           | 32.4                | 710   |
| Vevo3100  | MX250D     | LA                                       | 21                              |                   | 47 (2019)           | 23.9                | 512   |
| Vevo3100  | MX550D     | LA                                       | 40                              |                   | 43 (2019)           | 11.9                | 274   |

the remaining one by S-Sharp Co (Taipei, Taiwan). Of the 17 transducers tested, 9 of the transducers were single-element transducers and the remaining 8 were linear array transducers. Two EPPs were used to undertake the measurements, the second EPP was manufactured in 2015. The phantoms were cross-compared and measurements undertaken using the same transducers on different phantoms were within  $\pm 5\%$ .

The measurement procedure was identical for all transducers and made during scanner acceptance testing, within the loan period of a transducer or during visits to biological research facilities. Measurements were undertaken by the same operator in low ambient lighting similar to levels used when scanning live animals. For each transducer, three measurements of L were undertaken for each pipe diameter and the mean values from each pipe were plotted to form a resolution integral curve (**Figure 1**).

The performance of three of the Vevo 770 single element transducers were monitored annually over the 10 years period from 2010 to 2020. For the Vevo 770 scanner and Vevo 3100 scanner, annual maintenance checks were undertaken and software was upgraded as prescribed by the manufacturer. For the remaining preclinical scanners and transducers, measurements were undertaken as single measurements and no information was sought on maintenance or software status.

## RESULTS

**Table 1** shows the 17 commercially available transducers that were assessed. Data for five of the single element transducers and

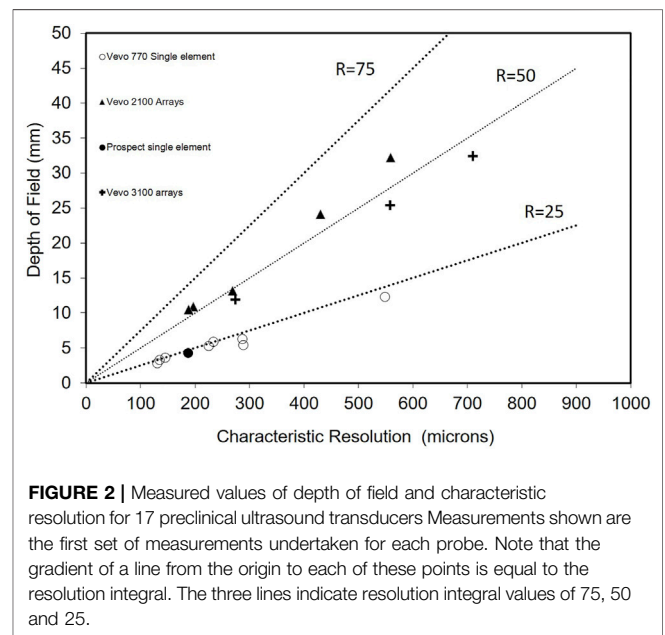


**FIGURE 2** | Measured values of depth of field and characteristic resolution for 17 preclinical ultrasound transducers. Measurements shown are the first set of measurements undertaken for each probe. Note that the gradient of a line from the origin to each of these points is equal to the resolution integral. The three lines indicate resolution integral values of 75, 50 and 25.

the Vevo 2100 transducers have previously been reported [14] but we include the data here for completeness. This is the first time we report on data from the single element transducers RMV 716, RMV 703 and RMV 712, the Prospect imaging transducer, PB406 (S-Sharp, New Taipei City, Taiwan) and the three linear array Vevo 3100 transducers.

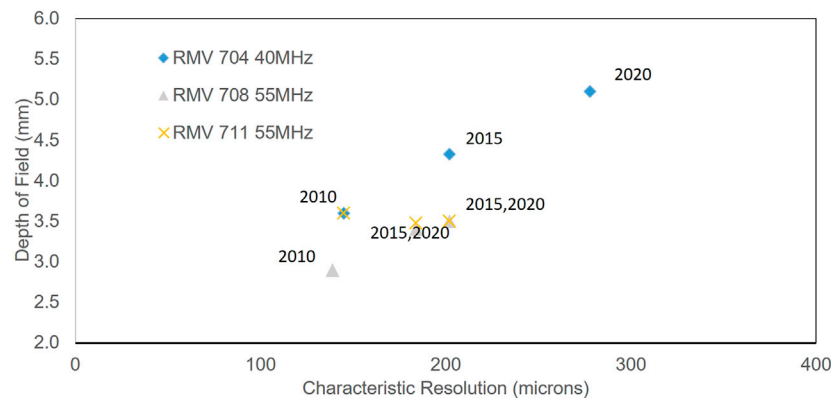


**FIGURE 3** | Measured values of depth of field and characteristic resolution for three single element preclinical transducers. Data shows results of measurements undertaken in 2010, 2015 and 2020.

**Figure 2** shows the depth-of-field versus characteristic resolution values for all transducers. Note that the gradient of the line connecting each data-point to the origin is equal to the resolution integral since  $R = L_R/D_R$ . All the array transducers have resolution integral values close to  $R = 50$  while single element transducers have  $R$  values close to 25. In **Supplementary Figures S1, S2** the characteristic resolution and depth-of-field are shown as a function of centre frequency, with smaller (better) characteristic resolution values and smaller depths-of-field associated with higher frequencies. Very similar depths-of-field are recorded for array transducers of the same nominal centre frequency and also for single element probes of the same nominal centre frequency. **Table 1** and **Figure 3** show the measured values of depth-of-field and characteristic resolution for three single element probes measured over a 10 years period with all three probes showing a shift in characteristic resolution to larger values and an increase in depth-of-field.

## DISCUSSION

Commercial test objects are routinely used to objectively assess ultrasound image performance to ensure that clinical ultrasound scanners perform to a predefined standard, to underpin decision making processes for replacement of equipment and as a versatile tool for the assessment of new imaging technologies [7]. For preclinical scanning, test objects have a similar role as changes in imaging performance, especially when gradual rather than a step-change, can result in significant degradation in image quality, spatial resolution and contrast resolution. Such degradation in the performance of ultrasound scanners can adversely affect the accuracy and reproducibility of the measurements acquired and increase the number of animals required to sufficiently power preclinical studies.

In this study, the imaging performance of 17 preclinical ultrasound transducers have been assessed with three transducers assessed over a period of 10 years.

From **Table 1** and **Figure 2**, resolution integral values for single element transducers ranged from 18 to 25 with the three

previously untested transducers demonstrating values similar to the single element transducers which had previously been measured.

From **Table 1**, characteristic resolution of the single element transducers varied by a factor of four from the 131  $\mu\text{m}$  of the RMV708 transducer with a nominal centre frequency of 55 MHz to the 549  $\mu\text{m}$  of the RMV716 transducer with a nominal centre frequency of 17.5 MHz. Despite this relatively wide range of characteristic resolution values, there was a relatively small spread of  $R$  values (18–25). For the array transducers,  $R$  values ranged from 43 to 58, and were approximately a factor of two greater than the single element transducers, indicating the improved imaging performance of these transducers. For these array transducers, characteristic resolution values varied approximately by a factor of three from 188  $\mu\text{m}$  of the MS550S transducer with nominal centre frequency of 40 MHz–710  $\mu\text{m}$  of the MX201 with a nominal centre frequency of 15 MHz.

**Supplementary Figures S1, S2** show the characteristic resolution and depth-of-field respectively as a function of frequency for both single element and array transducers. From **Supplementary Figure S2**, comparing the 40 MHz single element transducers (RMV704, PB406) to the array probes centred at 40 MHz (MS550D, MS550S, MX550D), it can be seen that the single element transducers exhibited smaller depth of field values compared to array transducers of the same nominal centre frequency. This is due to the stronger focusing at a fixed depth of the single element transducers compared to the dynamic focussing of the array probes. This extended depth of field with array transducers is also evident when scanning small animals. Over the limited depth-of-field of a single element transducer, small objects can be easily resolved (low characteristic resolution) and the transducer performs well. However, outwith the depth-of-field, the ability to resolve objects rapidly decreases and it is necessary to use transducers of different depth-of-fields or acoustic stand-offs. More details of this technique can be found elsewhere [15]. Using an array probe, multiple focal zones can be pre-selected, to optimise the image, extending the depth over which there is optimal characteristic

resolution. This shift in scanner development from single-element transducer technology to array-based transducer technology follows the same development path that was undertaken for transducers for clinical imaging where single element transducers commonly used in the 1980s and early 1990s were replaced by array transducers which are now used in almost all areas of clinical practice [16].

The imaging performance of two single element transducers with nominal centre frequencies at 35 MHz (RMV 703 and RMV 712), two at 40 MHz (RMV 704 and PB406) and two at 55 MHz (RMV 711 and RMV 708) were measured. For the two probes at 35 MHz, the RMV 712 had a focal length of 9 mm and the RMV 703 had a focal length of 10 mm. For these two probes, there was limited difference in depth of field measurements (5.9 vs. 6.3 mm—6.3% change) but improved characteristic resolution for the probe with shorter focal-length (234 vs. 287  $\mu\text{m}$ —18%). This improved characteristic resolution for probes with shorter focal-lengths was also seen for the two probes with nominal centre frequencies at 40 and 55 MHz.

In **Table 1** and **Figure 3** the change in R, characteristic resolution and depth-of-field values for three single element transducers are shown over a 10 years period, with measurements undertaken in 2010, 2015 and 2020. The two 55 MHz probes (RV711 and RMV708) were used infrequently over the 10 years and had the smallest change in R,  $L_R$  and  $D_R$  with insignificant change in the parameters occurring over the second 5 years. The RMV704 probe was used routinely over the period and displayed both an increase in depth of field (19%) and characteristic resolution (39%) over the initial 5 years period. This was noted as a gradual deterioration in image quality when scanning mice. The change over the second 5 years was a step-change in imaging performance which predominantly occurred over the period of 1 week, with a further deterioration in resolution integral and characteristic resolution of 14 and 18%, respectively. Interestingly for this probe and also for the RMV 708 probe, over the 10-years period, as the characteristic resolution values increased, the depth-of-field measurements were also found to increase suggesting that the focusing capability of the probes were deteriorating over time.

## CONCLUSION

Measurements of resolution integral, characteristic resolution and depth-of-field have been carried out on 17 commercially available high frequency preclinical ultrasound transducers using the Edinburgh Pipe Phantom. The transducers incorporated both single element and array technology and the measurements were carried out over a period ranging from 2008 to 2020. In addition, measurements from three of these transducers were undertaken

over a 10-year period. Our results demonstrate that array transducers tend to have R values approximately a factor of 2 greater than single element transducers demonstrating their enhanced performance over greater depths. In addition, single element transducers demonstrated smaller depth-of-field values and enhanced characteristic resolution values compared to array probes of the same frequency. Over a 10-years period, R values were found to decrease and characteristic resolution values increased, indicating a decrease in imaging performance of the probe. For some probes an increase in depth-of-field measurements was also observed. This work, demonstrates that R and its associated parameters, measured using the Edinburgh Pipe Phantom can be used to assess, track and quantitatively compare the imaging performance of preclinical ultrasound transducers. Moreover consistent use of the EPP enabled a means of reliably undertaking quality assurance testing of the preclinical scanners over the period, ensuring that transducers not fit-for-purpose were identified and providing data to underpin justification for replacement transducers and scanners.

## DATA AVAILABILITY STATEMENT

The raw data supporting the conclusions of this article will be made available by the authors, without undue reservation.

## AUTHOR CONTRIBUTIONS

CM undertook the measurements and wrote the paper. CM and KM designed and manufactured the test-objects. AT and SI reviewed the manuscript. SP designed the Edinburgh Pipe Phantom and reviewed the manuscript.

## ACKNOWLEDGMENTS

The authors wish to acknowledge Stan Loneskie, Bill Ellis, Anna Janeczko and Kirsty McNeil for their assistance. The authors wish to acknowledge funding from The Wellcome Trust—Grant Number 212923/Z/18/Z and CRUK—Grant Number A23333/24730.

## SUPPLEMENTARY MATERIAL

The Supplementary Material for this article can be found online at: <https://www.frontiersin.org/articles/10.3389/fphy.2022.802588/full#supplementary-material>

## REFERENCES

1. Browne JE, Ramnarine KV, Watson AJ, Hoskins PR. Assessment of the Acoustic Properties of Common Tissue-Mimicking Test Phantoms.

*Ultrasound Med Biol* (2003) 29:1053–60. doi:10.1016/s0301-5629(03)00053-x

2. Cannon LM, Fagan AJ, Browne JE. Novel Tissue Mimicking Materials for High Frequency Breast Ultrasound Phantoms. *Ultrasound Med Biol* (2011) 37: 122–35. doi:10.1016/j.ultrasmedbio.2010.10.005

3. Filoux E, Mamou J, Aristizabal O, Ketterling JA. Characterization of the Spatial Resolution of Different High-Frequency Imaging Systems Using a Novel Anechoic-Sphere Phantom. *IEEE Trans Ultrason Ferroelect Freq Contr* (2011) 58:994–1005. doi:10.1109/tuffc.2011.1900
  4. Joy J, Riedel F, Valente A, Cochran S, Corner G. Automated Performance Assessment of Ultrasound Systems Using a Dynamic Phantom. *Ultrasound* (2014) 22:199–204. doi:10.1177/1742271x14549591
  5. Pye SD, Ellis W. The Resolution Integral as a Metric of Performance for Diagnostic Grey-Scale Imaging. *J Phys Conf Ser* (2011) 279:012009. doi:10.1088/1742-6596/279/1/012009
  6. McGillivray TJ, Ellis W, Pye SD. The Resolution Integral: Visual and Computational Approaches to Characterising Ultrasound Images. *Phys Med Biol* (2010) 55:5067–88. doi:10.1088/0031-9155/55/17/012
  7. Moran CM, Inglis S, McBride K, McLeod C, Pye SD. The Imaging Performance of Diagnostic Ultrasound Scanners Using the Edinburgh Pipe Phantom to Measure the Resolution Integral - 15 Years of Experience. *Ultraschall Med* (2020) (efirst). doi:10.1055/a-1194-3818
  8. Inglis S, Janeczko A, Ellis W, Plevris JN, Pye SD. Assessing the Imaging Capabilities of Radial Mechanical and Electronic Echo-Endoscopes Using the Resolution Integral. *Ultrasound Med Biol* (2014) 40:1896–907. doi:10.1016/j.ultrasmedbio.2014.02.009
  9. McLeod C, Moran CM, McBride KA, Pye SD. Evaluation of Intravascular Ultrasound Catheter-Based Transducers Using the Resolution Integral. *Ultrasound Med Biol* (2018) 44:2802–12. doi:10.1016/j.ultrasmedbio.2018.07.014
  10. Wang S, Herbst EB, Pye SD, Moran CM, Hossack JA. Pipe Phantoms with Applications in Molecular Imaging and System Characterization. *IEEE Trans Ultrason Ferroelect Freq Contr* (2017) 64(1):39–52. doi:10.1109/tuffc.2016.2626465
  11. Ramnarine KV, Anderson T, Hoskins PR. Construction and Geometric Stability of Physiological Flow Rate Wall-Less Stenosis Phantoms. *Ultrasound Med Biol* (2001) 27:245–50. doi:10.1016/s0301-5629(00)00304-5
  12. Sun C, Pye SD, Browne JE, Janeczko A, Ellis B, Butler MB, et al. The Speed of Sound and Attenuation of an IEC Agar-Based Tissue-Mimicking Material for High Frequency Ultrasound Applications. *Ultrasound Med Biol* (2012) 38:1262–70. doi:10.1016/j.ultrasmedbio.2012.02.030
  13. Rajagopal S, Sadhoo N, Zeqiri B. Reference Characterisation of Sound Speed and Attenuation of the IEC Agar-Based Tissue-Mimicking Material up to a Frequency of 60 MHz. *Ultrasound Med Biol* (2015) 41:317–33. doi:10.1016/j.ultrasmedbio.2014.04.018
  14. Moran CM, Ellis W, Janeczko A, Bell D, Pye SD. The Edinburgh Pipe Phantom: Characterising Ultrasound Scanners Beyond 50 MHz. *J Phys Conf Ser* (2011) 279:012008. doi:10.1088/1742-6596/279/1/012008
  15. Moran CM, Pye SD, Ellis W, Janeczko A, Morris KD, McNeilly AS, et al. A Comparison of the Imaging Performance of High Resolution Ultrasound Scanners for Preclinical Imaging. *Ultrasound Med Biol* (2011) 37:493–501. doi:10.1016/j.ultrasmedbio.2010.11.010
  16. Moran CM, Inglis S, Pye SD. The Resolution Integral - A Tool for Characterising the Performance of Diagnostic Ultrasound Scanners. *Ultrasound* (2014) 22:37–43. doi:10.1177/1742271x13518202
- Conflict of Interest:** The authors declare that the research was conducted in the absence of any commercial or financial relationships that could be construed as a potential conflict of interest.
- Publisher's Note:** All claims expressed in this article are solely those of the authors and do not necessarily represent those of their affiliated organizations, or those of the publisher, the editors and the reviewers. Any product that may be evaluated in this article, or claim that may be made by its manufacturer, is not guaranteed or endorsed by the publisher.
- Copyright © 2022 Moran, McLeod, McBride, Inglis, Thomson and Pye. This is an open-access article distributed under the terms of the Creative Commons Attribution License (CC BY). The use, distribution or reproduction in other forums is permitted, provided the original author(s) and the copyright owner(s) are credited and that the original publication in this journal is cited, in accordance with accepted academic practice. No use, distribution or reproduction is permitted which does not comply with these terms.